

# A NOVEL DC-LINK VOLTAGE CONTROL STRATEGY FOR SHUNT ACTIVE POWER FILTERS USING SLIDING MODE CONTROLLER

<sup>1</sup>KUSHAL BORAGE, <sup>2</sup>SEEMA DIWAN

<sup>1</sup>PG Student, Department of Electrical Engineering, Walchand College of Engineering Sangli, Maharashtra.  
<sup>2</sup>Assistant Professor, Department of Electrical Engineering, Walchand College of Engineering, Sangli, Maharashtra.  
E-mail: <sup>1</sup>kushalvborage1993@gmail.com, <sup>2</sup>seema.diwan@walchandsangli.ac.in

---

**Abstract** - A sudden load variations influence the operation of shunt active power filter (APF). This paper proposes a novel DC-link voltage control strategy to reduce this drawback. In this control scheme, capacitor voltage is controlled by technique which involves both standard PI and sliding mode controllers. The gain of PI controller is regulated continuously by sliding mode controller depends on loop error and derivative. Transition rule is used to reduce the chattering phenomenon which is mainly caused by sliding mode controller. This controller is termed as SMPI.

Shunt APF is implemented without harmonic detection schemes in which the phase currents of grid are indirectly regulated to avoid reference frame transformation. The realization of the system is implemented by using MATLAB/Simulink. Comparison of performances of SMPI and conventional PI controller is also shown. Simulation result proves SMPI is more effective than conventional PI controller.

---

**Keywords** - Active Power Filter (APF), Proportional Integral (PI), Sliding Mode Proportional Integral (SMPI), Voltage Source Inverter (VSI).

---

## I. INTRODUCTION

Thyristors and other semiconductor switches are employed to feed controlled electric power to electrical loads in ac systems, such as furnaces, adjustable speed drives etc. Such nonlinear loads draw harmonic and reactive power components of current from ac mains which cause low system efficiency, interference in nearby communication networks, disturbances to other consumers [1]. There are many solutions to solve these problems. Conventional solution is passive filters for reducing the current harmonic [2].

The drawback of passive filter is overcome by active filter. Shunt APF is used for reactive power compensation, harmonics elimination etc. Control schemes applied to shunt APF are based on harmonic extraction from load side such as d-q method, p-q theory, adaptive filters, wavelet and artificial neural network and its effectiveness is depends on quickly and accurately identification of the harmonic components present in nonlinear load. The shunt APF can also be implemented without taking load harmonic i.e. based on balanced energy method. In this method, system active power is balanced to obtain harmonic compensating term and its effectiveness depends on how fast system reaches equilibrium state [3]. PI controller is used for controlling capacitor voltage of shunt APF in load harmonic extraction method as well as balanced energy method. Some alternatives to improves shunt APF DC-link performance have been proposed, such as the feed forward schemes for compensating the power grid voltage fluctuations [4] in which the voltage amplitude fluctuation of the supply and the compensation current fluctuation can cause the fluctuation in shunt APF dc-link capacitor voltage.

Another method is the use of adaptive control techniques for flexibility of reactive compensation in hybrid active power filters [5] in which the dc-link voltage as well as the reactive power compensation range can be changed according to different inductive loading situations.

The proposed control strategy is use to improve performance of shunt APF during severe load changes based on balance energy method. In this control scheme, capacitor voltage is controlled by technique which involves both standard PI and sliding mode controllers. The gain of PI controller is regulated continuously by sliding mode controller depends on loop error and derivative. Transition rule is used to reduce the chattering phenomenon which is mainly caused by sliding mode controller. This controller is termed as SMPI. Shunt APF is implemented without harmonic detection schemes in which the phase currents of grid are indirectly regulated to avoid reference frame transformation. The realization of the system is implemented by using MATLAB/Simulink. Comparison of performances of SMPI and conventional PI controller is also shown. Simulation result proves SMPI is more effective than conventional PI controller.

## II. SYSTEM AND ITS MODELING EQUATION

### A. System block diagram

Fig.1 shows the block diagram of shunt APF used in MATLAB/simulation. It consist of three-phase grid source with internal impedance ( $Z_m = r_m + j\omega L_m$ ) feeds to three-phase uncontrolled rectifier load ( $Z_{NL} = r_{NL} + j\omega L_{NL}$ ). Shunt APF is implemented with a VSI through impedance ( $Z_F = r_F + j\omega L_F$ ). The control system including sensors, drives is well executed in MATLAB simulation.

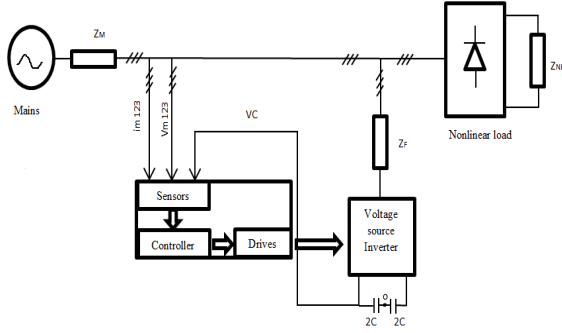


Fig.1 Basic block diagram of proposed shunt APF.

## B. Modeling of block diagram of shunt APF for simulation

Shunt APF system in which interaction of grid impedance with filter and load was studied in [3]. Therefore transfer function of the dynamics of power grid currents is shown in Eq. (1)

$$Bc(s) = \frac{I_{sdq}(s)}{V_{fdq}(s)} \cong -\frac{p_s}{s+q_s} \quad (1)$$

Where  $p_s = \frac{1}{l_F+l_m}$  and  $q_s = \frac{r_F+r_m}{l_F+l_m}$ . The value of  $p_s$  and  $q_s$  may vary when impedance of load and grid varies.

The modeling of electrolytic capacitors used in in DC-link of shunt APF is discussed in [6], [7]. Therefore resulting transfer function model is given by

$$Bv(s) = \frac{Vc(s)}{I_{sd}(s)} \cong \frac{p_c}{s+q_c} \quad (2)$$

Where  $p_c = \frac{1}{c}$  and  $q_c = \frac{1}{r_{pc}}$  C is the capacitance of electrolytic capacitor model and  $r_{pc}$  is resistance accounts for leakage current in capacitor.

## III. CONTROL DIAGRAM

Fig. 2 shows the Simulink block diagram of the proposed control strategy for shunt APF based on balanced energy method. In this Fig. 2, the DC-link voltage is controlled by SMPI controller. It generates the reference current  $i_{sd}^*$  which will helps to determine active power component of the system. 1-D lookup table block is used to give the different reference capacitor voltage to the controller. Phase locked loop is used to determine phase angle of the power grid  $\theta_s$ . The  $dq$  reference phase currents can be obtained by using equations (3) and (4).

$$i_{sd} = i_{sd}^* \cos(\theta_s) \quad (3)$$

$$i_{sq} = i_{sd}^* \sin(\theta_s) \quad (4)$$

The phase currents are indirectly regulated by two separate current controllers to avoid reference frame transformation. The block  $dqo$  to  $abc$  helps to transformation of reference frame to three phase

system. PWM block determines the duty ratio of voltage source inverter.

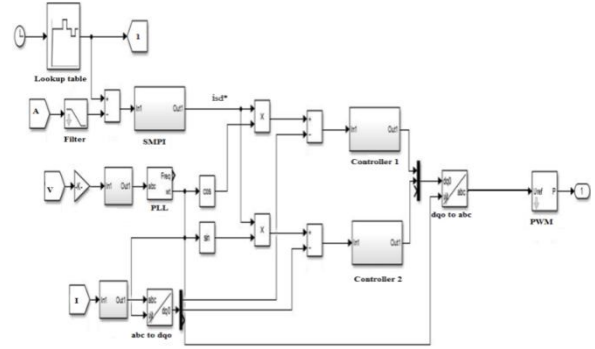


Fig.2 Simulink diagram of proposed control strategy.

## A. Current controller

The current controllers shown in Fig. 2 are used for regulating the grid currents and it is based on sequence control scheme. Therefore one controller is for positive and another for negative sequence which is discussed in [8]. The transfer function of the current controller can be given by Eq. (5).

$$I_c(s) = \frac{2k_{pc}s^2 + 2k_{ic}s + 2k_{pc}w_s^2}{s^2 + w_s^2} \quad (5)$$

Where  $k_{pc}$  and  $k_{ic}$  are the current controller gains and  $w_s$  is the fundamental frequency.

Design of current controller is based on zero-pole cancellation method. Thus, gains  $k_{pc}$  and  $k_{ic}$  as

$$q_s = \frac{k_{ic}}{k_{pc}} \quad (6)$$

Current controller band-pass frequency determined as  $p = p_s k_{pc}$ . Therefore  $q_s$  and  $p_s$  results in

$$k_{pc} = \frac{w_p}{p_s} \quad (7)$$

And

$$k_{ic} = \frac{q_s w_p}{p_s} \quad (8)$$

## B. Capacitor voltage controller

The proposed voltage control loop consists of SMPI controller which is implemented by proportional integral (PI) and sliding mode control scheme. The gain of PI controller is calculated by SM control approach in which it used control loop error and its derivative. Transition rule is used to reduce the chattering phenomenon which is mainly caused by sliding mode controller. SMPI controller transfer function is given by

$$x_v(s) = \frac{k_{ps} + k_i}{s} \quad (9)$$

Where  $k_p$  and  $k_i$  are the DC-link voltage controller gain which is determined by sliding mode control method. In this control method sliding surface is required therefore it defines as

$$s_s = de_v + e_v \quad (10)$$

Where,  $s_s$  is sliding surface,  $e_v = v_c^* - v_c$  and  $e_v'$  is its derivative and  $d$  is a positive constant.

SMPI is stable at origin ( $s_s = 0$ ), thus Lyapunov candidate be

$$L(e_v) = \frac{1}{2}e_v^2 \quad (11)$$

$$L(e_v) = e_v e_v' = -de_v^2 < 0 \quad (12)$$

Due to stability restrictions, the following switching laws decides controller gains

$$k_p = [(1 + \text{sgn}(s_s))k_p^1 - (1 - \text{sgn}(s_s))k_p^2] + k_p^3 \quad (13)$$

$$k_i = [(1 + \text{sgn}(s_s))k_i^1 - (1 - \text{sgn}(s_s))k_i^2] + k_i^3 \quad (14)$$

Where  $k_p^1$ ,  $k_p^2$ ,  $k_p^3$ ,  $k_i^1$ ,  $k_i^2$ , and  $k_i^3$  are positive constant and can be determined using standard PI design method. The math function  $\text{sgn}(s_s)$  gives 1 value when  $s_s > 0$  and -1 value when  $s_s < 0$ .

During transient state, the performance of SMPI is good but at steady state it gives undesired side effect. It is mainly due to the chattering produced by sliding mode control switching laws used to calculate gains of controller.

Therefore it can be avoid if controller gains fixed in steady state. So the transition rule is employed in control system.

Defining Gaussian function,

$$G(e_v) = e^{-\frac{e_v^2}{\epsilon}} \quad (15)$$

Where  $G$  is the decision parameter which decides between fixed controller and switching controller,  $e_v$  is capacitor voltage error and  $\epsilon$  is the parameter of Gaussian function.

In Fig.3, the value of  $G_t$  represents threshold value at which transition must occurred with respect to voltage error  $e_t$ . Transition operates as follows: the value of  $G(e_v)$  in Eq. (15) is continuously calculated for each value of  $e_v$ . If this value is less than  $G_t$ , the controller works as SMPI otherwise it works as fixed gain standard PI controller.  $\epsilon$  determines the smoothness of transition. If the value of  $\epsilon$  is higher,  $G$  is less sensitive to the voltage error. If the value of  $\epsilon$  is lower then  $G$  will more sensitive to the voltage error. The simulink block diagram of the SMPI controller is shown in Fig.4. In this controller,  $k_p$  and  $k_i$  are determined by switching laws given in Eq. (13) and (14). It is obtained from sliding surface design  $s_s$ .

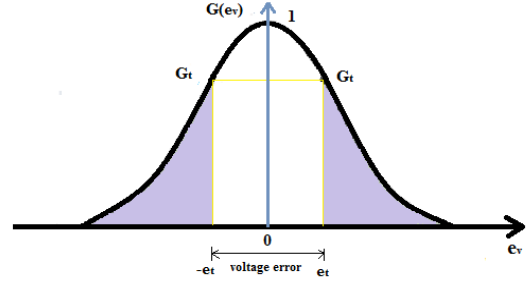


Fig.3 Transition rule G

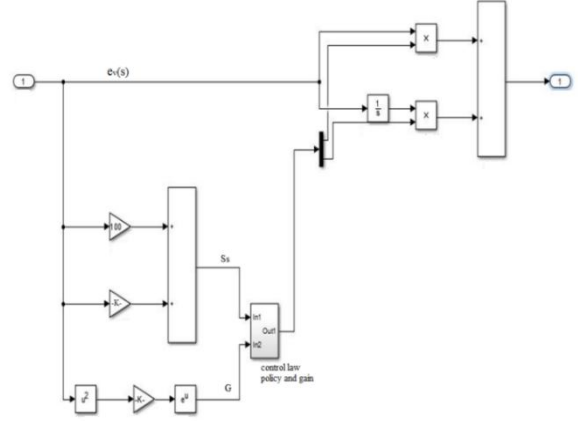


Fig.4 Simulink diagram of SMPI control scheme

## RESULTS AND DISCUSSION

The Simulink model of proposed shunt APF is shown in Fig.5. It is composed by three phase supply feeding a nonlinear load. The voltage source inverter is connected to system through input filter inductors  $lF=1.0\text{mH}$ . The capacitor is taken as  $2200\mu\text{F}$  with voltage  $410\text{V}$ . The nonlinear load is made by three phase uncontrolled rectifier feeding a RL load  $rNL=40\Omega$  and  $lNL=30\text{mH}$ . The signal taken from sensors is passing through low pass filter having cutoff frequency  $2.5\text{kHz}$ . The shunt APF parameters used in simulation are provided in Table I.

$V_s = 110\text{V (rms)}$	$F_s = 50\text{Hz}$
$rm = 0.2\Omega$	$lm = 0.1\text{mH}$
$rF = 2\Omega$	$lF = 1\text{mH}$
$rNL = 40\Omega$	$lNL = 30\text{mH}$
$C = 2200\mu\text{F}$	$F_{sw} = 10\text{kHz}$

Table I: Shunt APF simulation parameter

The SMPI controller parameters used in simulation are provided in Table II.

$k_p^1 = 0.033$	$k_p^2 = 0.022$	$k_p^3 = 0.11$
$k_i^1 = 2.145$	$k_i^2 = 0.88$	$k_i^3 = 2.75$

Table II: SMPI simulation parameter

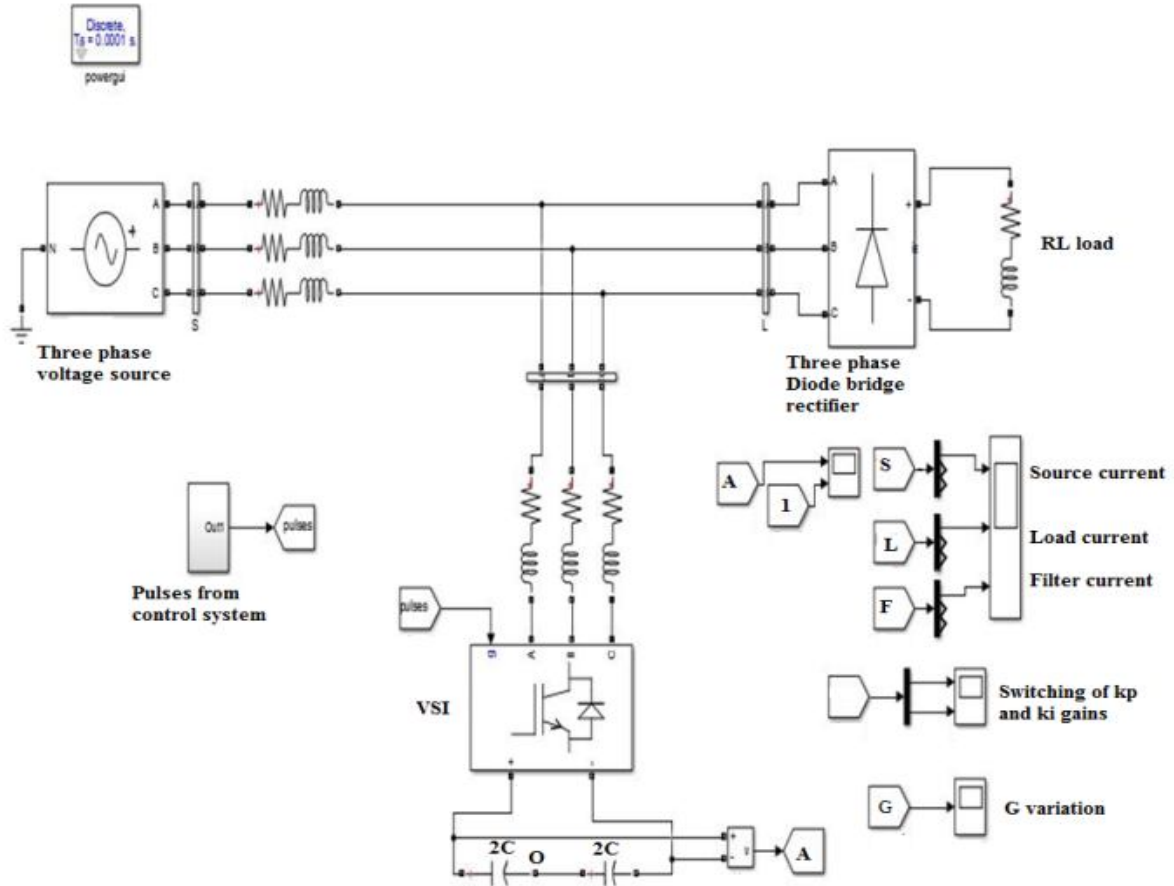


Fig.5 Simulink model of shunt APF

For sudden load variations a different conditions are considered in simulation. Also comparison of SMPI with conventional PI was done to highlight the benefits of SMPI technique. The following results were investigated: a) DC-link capacitor voltage during startup. b) DC-link capacitor voltage during step transients of its reference voltage. c) Load transients. d) THD after and before compensation.

Fig.6 shows that simulation result for DC-link capacitor voltage during start-up. Here both the controllers are compared with respect to reference ramp having slope of 346 V/s. The proposed controller SMPI is smoother, less response time, and less overshoot as compared to conventional PI.

Fig.7 shows a comparison for both controllers for variation of reference voltage. Proposed SMPI controller gives better results for DC-link capacitor voltage during step up and step down transients of its reference voltage. Fig.8 (a) shows a zoom of step up transient at  $t = 5\text{sec}$ . and Fig. 8 (b) shows a zoom of step down transient at  $t = 9\text{sec}$ . This reference voltage variation is only for comparison purpose. For actual working of shunt APF, constant reference voltage is considered.

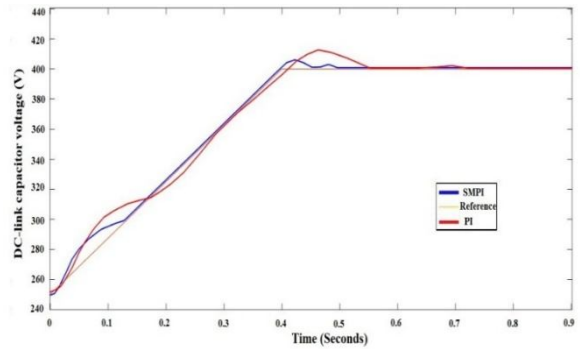


Fig.6 Simulation result for DC-link capacitor voltage during start-up

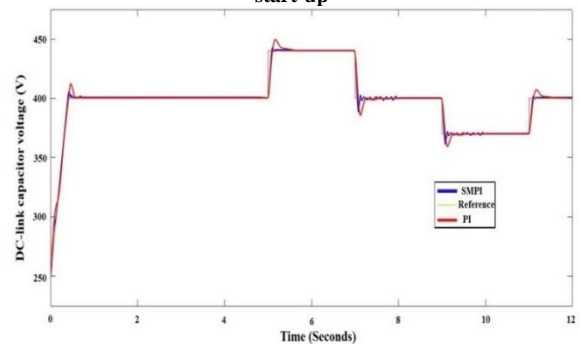
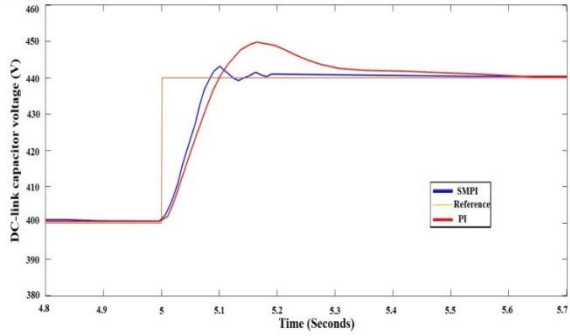
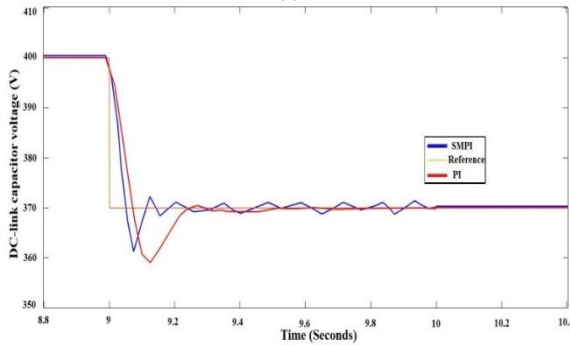


Fig.7 Simulation result for DC-link capacitor voltage during step up and step down transients of its reference voltage.



(a)



(b)

**Fig.8 Simulation result for DC-link capacitor voltage during (a) step up transient and (b) step down transient of its reference voltage.**

Fig.9 shows function G variation for the result presented in Fig. 7 and it is mostly used to avoid chattering. Fig 10 shows gain  $k_p$  and  $k_i$  variations for the result presented in Fig.7.

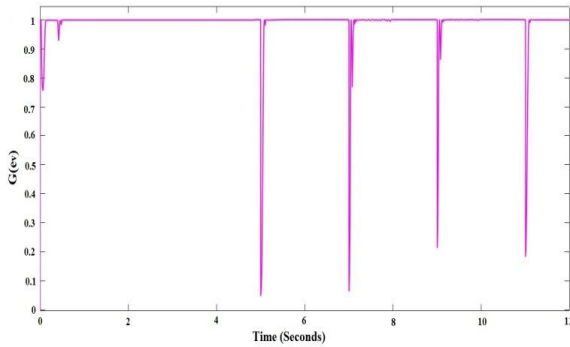
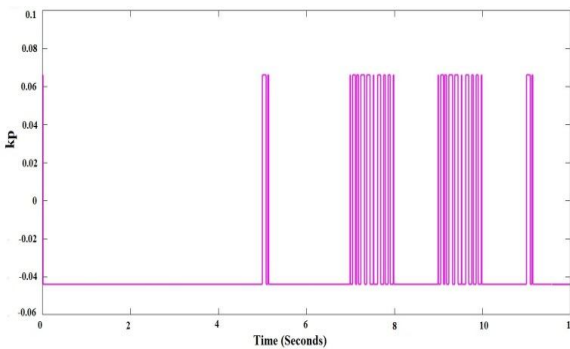
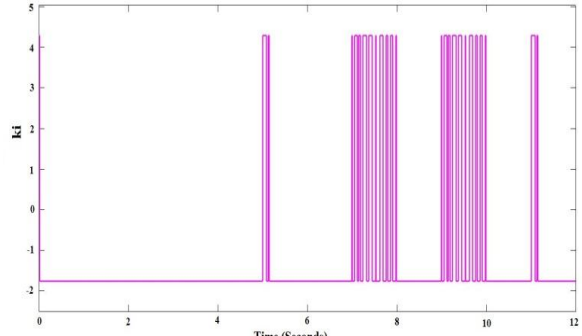


**Fig.9 Simulation result for function G used for transition.**

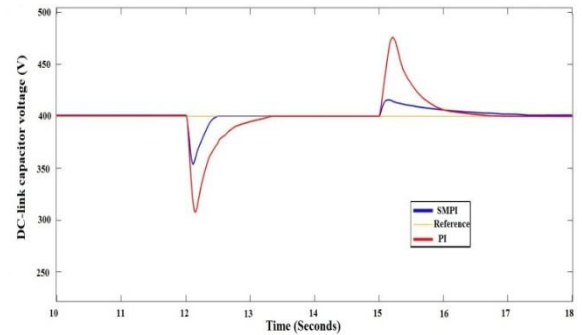


(a)

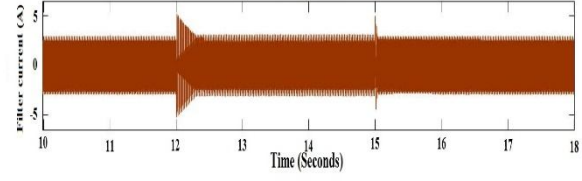
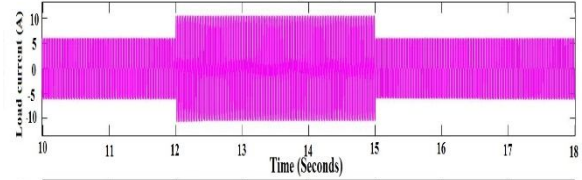
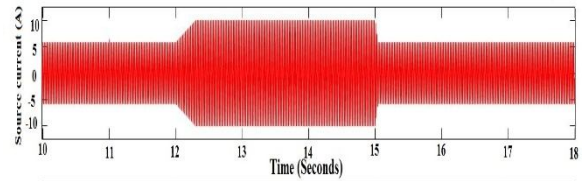


(b)

**Fig.10 Simulation result for gain (a)  $k_p$  and (b)  $k_i$**



(a)



(b)

**Fig.11 Simulation result during load transients (a) for DC-link capacitor voltage (b) for source, load and filter current.**

Now consider load transients presents in shunt APF applications. Fig. 11 shows load transients impacts on DC-link capacitor voltage, source current, load current and filter current. Fig. 12 shows function G variation during load transients. There are two variations are considered, first one is (Fig. 13) at  $t = 12\text{sec}$  in which load power increases with an additional ( $30\Omega$ ) three phase resistor is connected in parallel with nonlinear load. For this increased load transient, SMPI controller and conventional PI controller is compared. It is clearly shown that SMPI

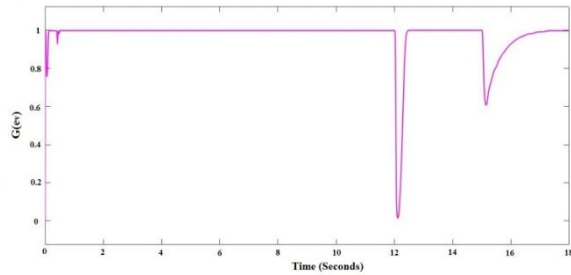


Fig.12 Simulation result for function G during load transients.

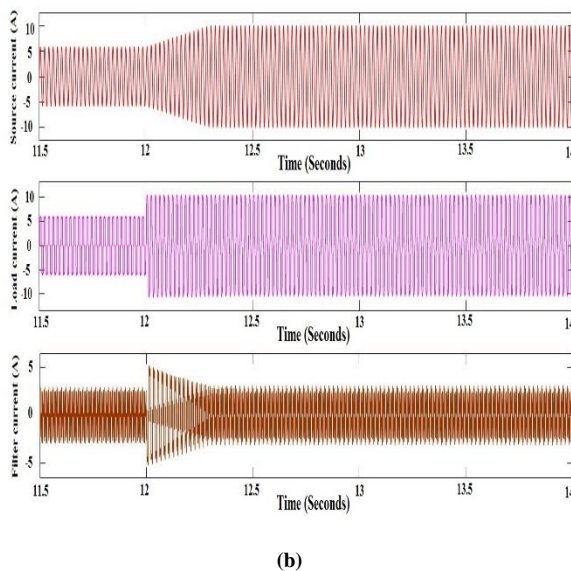
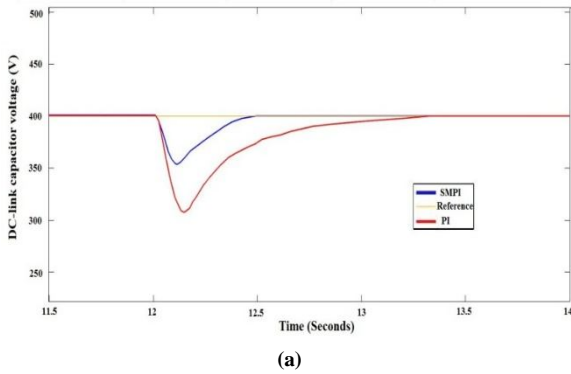


Fig.13 Simulation result during load power increase (a) for DC-link capacitor voltage (b) for source, load and filter current.

gives better performance than PI since SMPI and PI undershoot values are nearly 12% and 23% respectively. SMPI controller also gives better performance than PI when load power reduction is considered as shown in Fig. 14. Observed at  $t = 15\text{sec.}$  and this is obtained by disconnecting the additional resistive load. The grid phase currents are multiply by 10 and gridphase voltages are superimposed by its grid phase currents for proper presentation. The source current, load current and filter current waveforms after compensation are shown in Fig.15. With proposed control strategy, THD of the system before compensation is 29.27 % and after compensation is 1.02 %.

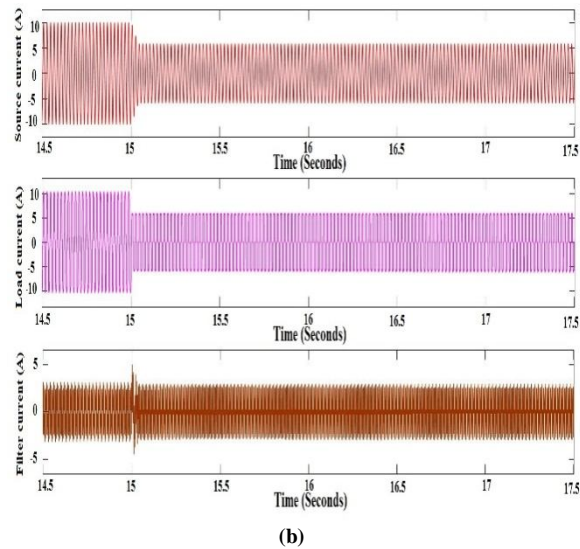
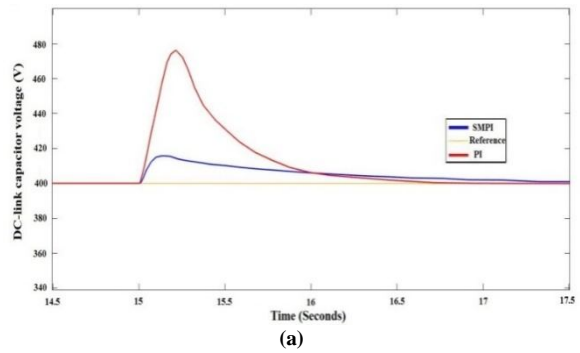


Fig.14 Simulation result during load power reduced (a) for DC-link capacitor voltage (b) for source, load and filter current.

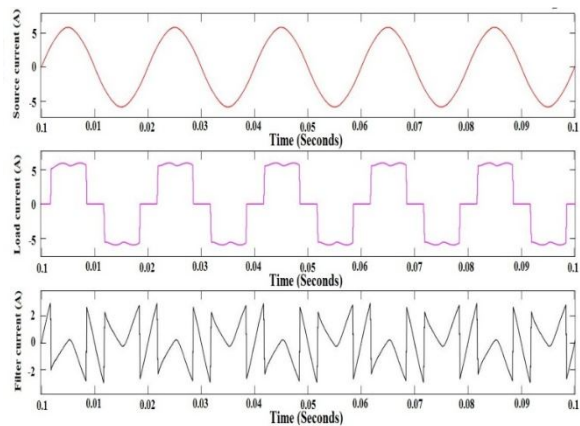


Fig.15 Simulation result of Source current, load current and filter current after compensation.

## CONCLUSION

The proposed control system is implemented by using MATLAB/Simulink. Hence a control approach proposed by this paper is improves the performance of shunt APF without measuring load currents, thus it will reduce the number of current sensors when it is performed experimentally. In this paper, DC-link voltage is controlled by SMPI controller in which sliding mode control approach is used to gain calculations. Transition rule is used to reduce the

chattering phenomenon which is mainly caused by sliding mode controller. Thus DC-link voltage control loop gives better performance during occurrence of sudden load variations. The comparison between SMPI and standard PI controller on the basis of performance is also shown. SMPI controller gives better performance for both load transients as well as step up and step down transients in DC-link reference voltage as compared to PI controller.

## REFERENCES

- [1] B. Singh, K. Al-Haddad, and A. Chandra, "A review of active filters for power quality improvements," *IEEE Trans. Ind. Electron.*, vol. 46, pp. 960–971, Oct. 1999.
- [2] R. Ribeiro, C. Azevedo, and R. Sousa, "A robust adaptive control strategy of active power filters for power-factor correction, harmonic compensation, and balancing of nonlinear loads," *IEEE Trans. Power Electron.*, vol. 27, pp. 718–730, Feb. 2012.
- [3] R. L. d. A. Ribeiro, T. d. O. A. Rocha, R. M. de Sousa, E. C. dos Santos and A. M. N. Lima, "A Robust DC-Link Voltage Control Strategy to Enhance the Performance of Shunt Active Power Filters Without Harmonic Detection Schemes," in *IEEE Transactions on Industrial Electronics*, vol. 62, no. 2, pp. 803-813, Feb. 2015.
- [4] W. Longhui, Z. Fang, Z. Pengbo, L. Hongyu, and W. Zhaoan, "Study on the influence of supply-voltage fluctuation on shunt active power filter,," *IEEE Trans. Power Delivery*, vol. 22, pp. 1743.1749, July 2007.
- [5] C.-S. Lam, W.-H. Choi, M.-C.Wong, and Y.-D. Han, "Adaptive dc-link voltage-controlled hybrid active power filters for reactive power compensation," *IEEE Trans. Power Electron.*, vol. 27, pp. 1758–1772, Apr. 2012.
- [6] M. Gasperi, "Life prediction modeling of bus capacitors in ac variable frequency drives," *IEEE Trans. Ind. Applicat.*, vol. 41, pp. 1430–1435, nov./dec. 2005.
- [7] A. Braham, A. Lahyani, P. Venet, and N. Rejeb, "Recent developments in fault detection and power loss estimation of electrolytic capacitors," *IEEE Trans. Power Electron.*, vol. 25, pp. 33–43, Jan. 2010.
- [8] C. Jacobina, M. Correa, R. Pinheiro, E. da Silva, and A. Lima, "Modeling and control of unbalanced three-phase systems containing pwm converters," *IEEE Trans. Ind. Applicat.*, vol. 37, pp. 1807–1816, nov./dec. 2001.

★ ★ ★